

Further studies of 1E 1740.7–2942 with *ASCA*

Masaaki Sakano¹, Kensuke Imanishi, Masahiro Tsujimoto, Katsuji Koyama²

Department of Physics, Kyoto University, Kyoto 606-8502 Japan,

sakano@cr.scphys.kyoto-u.ac.jp, kensuke@cr.scphys.kyoto-u.ac.jp,

tsujimot@cr.scphys.kyoto-u.ac.jp, koyama@cr.scphys.kyoto-u.ac.jp

and

Yoshitomo Maeda¹

Department of Astronomy and Astrophysics, Pennsylvania State University, University Park PA 16802-6305 U.S.A., maeda@astro.psu.edu

Received _____; accepted _____

¹Research Fellow of the Japan Society for the Promotion of Science.

²CREST: Japan Science and Technology Corporation (JST)

ABSTRACT

We report the *ASCA* results of the Great Annihilator 1E 1740.7–2942 obtained with five pointing observations in a time span of 3.5 years. The X-ray spectrum for each period is well fitted with a single power-law absorbed by a high column of gas. The X-ray flux changes by a factor of 2 from period to period, but the other spectral parameters show no significant change. The photon index is flat with $\Gamma = 0.9\text{--}1.3$. The column densities of hydrogen N_{H} is $\sim 1.0 \times 10^{23} \text{ H cm}^{-2}$ and that of iron N_{Fe} is $\sim 10^{19} \text{ Fe cm}^{-2}$. These large column densities indicate that 1E 1740.7–2942 is near at the Galactic Center. The column density ratio leads the iron abundance to be 2 times larger than the other elements in a unit of the solar ratio. The equivalent width of the $\text{K}\alpha$ -line from a neutral iron is less than 15 eV in 90% confidence. This indicates that the iron column density within several parsecs from 1E 1740.7–2942 is less than $5 \times 10^{17} \text{ Fe cm}^{-2}$. In addition, the derived hydrogen column density is about 1/6 of that of giant molecular clouds in the line of sight. All these facts support that 1E 1740.7–2942 is not in a molecular cloud, but possibly in front of it; the X-rays are not powered by accretion from a molecular cloud, but from a companion star like ordinary X-ray binaries.

Subject headings: accretion, accretion disks — black hole physics — stars: individual (1E 1740.7–2942) — X-rays: stars — ISM: clouds

1. Introduction

The center of our Milky Way Galaxy is one of the most complex regions in X-rays as well as the other wave bands. In fact, many X-ray point sources, including transients, have been detected with the past observations. Among these, 1E 1740.7–2942 has been found to be quite unusual. This source was discovered with the *Einstein*/IPC in the soft X-ray band below 3.5 keV (Hertz & Grindlay 1984). Higher energy observations revealed an unusually hard spectrum (Skinner et al. 1987, 1991; Kawai et al. 1988; Cook et al. 1991; Bazzano et al. 1992; Cordier et al. 1993a, 1993b; Goldwurm et al. 1994). In fact, this is by far the brightest source within a few degree of the Galactic Center in the high energy band above 20 keV with a power-law spectrum extending up to 100 keV or higher. It showed flux variability in the time scale from a day to a few years (Bouchet et al. 1991; Sunyaev et al. 1991; Churazov et al. 1993a, 1993b; Paciesas et al. 1993; Pavlinsky, Grebenev, & Sunyaev 1994; Zhang, Harmon, & Liang 1997). Variability of time scale shorter than a day has been detected by Smith et al. (1997). The spectral shape has been almost stable in time, regardless of the flux variations. These spectra and time variabilities generally resemble those of Cygnus X-1 (e.g., Kuznetsov et al. 1997), the prototype of the galactic black hole candidate. Unlike Cygnus X-1, however, optical and IR observations have failed to find any companion stars (Prince et al. 1991; Mereghetti et al. 1992; Djorgovski et al. 1992), probably due to strong extinction to the direction of the Galactic Center.

The electron-positron annihilation line at 511-keV from this source was reported with the *Granat*/SIGMA observations, hence 1E 1740.7–2942 has been referred to as the “Great Annihilator” (Bouchet et al. 1991; Sunyaev et al. 1991; Churazov et al. 1993b; Cordier et al. 1993a). Jung et al. (1995), Harris, Share, & Leising (1994a, 1994b), Malet et al. (1995), Smith et al. (1996), Cheng et al. (1998), on the other hand, reported no evidence for the annihilation line, making this issue debatable. The VLA radio observations revealed that 1E 1740.7–2942 has a radio counterpart with variable flux correlated to the X-ray variation (Mirabel et al. 1992, 1993). They also found non-thermal double jet-like structures emanating from the source, which resemble those of the galactic superluminal jet sources (e.g., Fender, Burnell, & Waltman 1997). Hence this source is also referred to as a “micro quasar”. These facts altogether place 1E 1740.7–2942 to be one of the best candidates of stellar mass black holes.

The CO observations found a giant molecular cloud whose density peak is in agreement with the position of 1E 1740.7–2942 (Bally & Leventhal 1991; Mirabel et al. 1991). They proposed that 1E 1740.7–2942 is an isolated or a binary black hole, powered directly from a surrounding molecular cloud such as by the Bondi-Hoyle accretion (Bondi & Hoyle 1944), although the conventional binary scenario with mass accretion from a companion star cannot be excluded.

X-ray spectrum and time variability would be keys for the study of the nature and emission mechanisms. In particular, the equivalent width of fluorescent iron line as a

function of absorption column provides direct evidence whether the source is really in a dense cloud or not. Churazov, Gilfanov, & Sunyaev (1996) and Sheth et al. (1996) have examined the X-ray spectra of this source with the Performance Verification (PV) and AO-2 phases of the early *ASCA* operations. Their derived N_{H} values, hence the conclusions, are not fully consistent with each other. This is partly due to the fact that they fitted the spectra with different energy range. More serious problem for the detailed spectral study of this source, particularly on the iron line, iron K-edge and low energy absorption structures, is possible contamination of the thin thermal Galactic plasma emission which includes strong emission lines (Koyama et al. 1996). Thus we have made further observations in AO-3 and AO-5 phases after the PV and AO-2, analyzed all the available data sets, putting our particular effort to remove properly the possible contamination from the plasma emission in the Galactic Center region. We assume the distance of the Galactic Center to be 8.5 kpc.

2. Observations

ASCA observations of 1E 1740.7–2942 were made on the five occasions, which are listed in Table 1. Two sets of the Solid-State Imaging Spectrometers (SISs) were operated in parallel with the Gas Imaging Spectrometers (GISs), both located separately at foci of four identical thin-foil X-ray telescopes (XRTs). Details of this instrumentation are found in Serlemitsos et al. (1995), Burke et al. (1991, 1994), Yamashita et al. (1997), Ohashi et al. (1996), Makishima et al. (1996), while a general description of *ASCA* can be found in Tanaka, Inoue, & Holt (1994).

In the PV and AO-2 observations, 1E 1740.7–2942 was pointed near the center of the field of view, while for the other observations, 1E 1740.7–2942 was out of the SIS field of view. In addition, we have made 8 sequential pointing observations near the Galactic Center with 20 ksec exposure for each. These series of observations covered the Galactic Center region of about 1×1.5 degree 2 and the data were used to estimate the Galactic diffuse background (see Sec. 3.3). Table 1 summarizes the observation log. Data reduction and cleaning were made with the standard method as described in the user guide by NASA Goddard Space Flight Center (GSFC). The event selection and the analysis were performed on UNIX workstations with the FTOOLS and XANADU packages released from the NASA GSFC.

EDITOR: PLACE TABLE 1 HERE.

3. Results and Analysis

3.1. X-ray images

The GIS mosaic images for the hard X-ray band (3–10 keV) and the soft X-ray band (0.7–1.5 keV) are given in Figure 1a and 1b, respectively. We find a strong point source at the *ROSAT* position of 1E 1740.7–2942 (($17^{\text{h}}43^{\text{m}}54^{\text{s}}.8$, $-29^{\circ}44'38''$) in J2000 coordinate (Heindl, Prince, & Grunsfeld 1994)), within the nominal *ASCA* error circle of about 1' radius in each image. The excess X-ray flux above the diffuse background level is higher in the hard X-ray band than that in the soft band. This immediately indicates that either the X-rays are highly absorbed, or the spectrum is very hard, or probably both.

We also find a faint soft source, AX J1744.3–2940, at ($17^{\text{h}}44^{\text{m}}18^{\text{s}}$, $-29^{\circ}40'1$) in J2000 coordinate with the error circle of about 1'. This position is in good coincidence with the source 2 in Heindl et al. (1994) observed with *ROSAT*, or 1WGA J1744.2–2939. It is about 7' offset from 1E 1740.7–2942, hence the photon contamination from this source for the analysis of 1E 1740.7–2942 is negligible.

EDITOR: PLACE FIGURE 1 HERE.

3.2. Light curves

Since the X-rays from 1E 1740.7–2942 are limited to above about 2 keV (see next section or X-ray images in Figure 1), we made light curve for each observation, accumulating 2–10 keV photons in the circular region within 3' radius from the source. To increase statistics, we summed the data of SIS 0 and 1, or GIS 2 and 3 with a time bin of 256 sec. As an example, we show the light curves of the AO-2 1st observation in Figure 2. Constant flux assumption for the light curve of each observation is rejected by χ^2 -tests with more than 90% confidence. Thus the X-ray flux was found to be variable although the variability amplitude is not large.

We also examined FFT analysis for the GIS 2+3 data of high-bit rate with 1/16 sec time resolution, and found no periodic variation in the time scale of 1/16 – 1000 second from any of the five separate observations.

As for the long term variability, we found the averaged flux in PV phase decreased to about 75% and 50% in AO-2 and AO-3 phases, respectively, and then increased in AO-5 phase to about the same flux as in PV phase (see Figure 4 and Sec. 3.3).

EDITOR: PLACE FIGURE 2 HERE.

3.3. Spectral Analysis

1E 1740.7–2942 is located near the Galactic Center region, which is filled with a high temperature plasma. The plasma emits diffuse X-rays including strong iron lines, with significant flux variations from position to position (Koyama et al. 1996). Therefore the spectrum of 1E 1740.7–2942 may be contaminated by the diffuse X-rays, especially in the low energy band and in the iron line feature.

To minimize possible effect to the spectrum due to the background variation, we accumulated the source X-ray photons in a small circle of 2' radius and extracted the background taken from the annulus of 2'–4' radius. We thus made the background subtracted spectra with GIS2+3 and SIS0+1 for each observation phase. For the AO-3 data, we excluded the region closely near to the detector edge or the calibration isotope from the background region.

We fitted each spectrum with an absorbed power-law, using the photo-electronic cross-sections by Bałucińska-Church & McCammon (1992). The abundances for the absorbing matters were fixed to the solar values (Anders & Grevesse 1989), but that of iron was allowed to be varied, because the 7.1-keV edge structure carries unique information of the iron column. Examples (AO-2) of the spectra with the best-fit models are given in Figure 3 and the best-fit parameters for all the observations are listed in Table 2.

We then fitted the GIS and the SIS data for each phase simultaneously with a power-law model. The results with the best statistics are also given in Table 2. The best-fit photon index is in the range of 0.9–1.3, the hydrogen column density is $(8\text{--}11)\times 10^{22}$ H cm^{−2}, and the iron abundance is found to be about 2 solar.

Although we found no clear emission line in each spectrum, we included a 6.4 keV line for the further fitting, because the emission line from neutral iron at 6.4 keV gives direct information around the cold gas near 1E 1740.7–2942. In this fitting we fixed the line energy and the intrinsic width to be 6.4 keV and 0 keV, respectively. The resultant parameters are listed in Table 2 together with the 2–10 keV flux (absorption included).

EDITOR: PLACE TABLE 2 HERE.

EDITOR: PLACE FIGURE 3 HERE.

In Figure 4, we summarize the long term spectral behavior. No significant difference, except for the flux change, is found from observation to observation in a time span of 3.5 years. In addition, the spectral slope is rather flat. Thus we can conclude that 1E 1740.7–2942 has been in the hard state of the galactic black hole spectrum.

EDITOR: PLACE FIGURE 4 HERE.

Since the galactic black hole candidates often have a soft component with temperature of less than 1.0 keV (e.g., Tanaka & Lewin 1995; van Paradijs 1998), we examined whether the 1E 1740.7–2942 spectrum requires a soft component or not. We tried to fit the data with a power-law model adding a soft black body component, and found no significant improvement by this procedure, hence the spectrum requires no soft component. However it is not clear whether this is real or merely due to large absorption in the low energy band.

The Galactic diffuse emission includes strong iron K-shell lines from neutral (at 6.4 keV) and highly ionized irons (at 6.7 keV and 6.97 keV) (Koyama et al. 1996; Maeda 1998). Since the K-shell line of a neutral iron (6.4 keV) plays a key role for the nature of 1E 1740.7–2942, we estimated the fluctuation of the diffuse K-shell lines (the 6.4 keV-lines) in the source extraction region, using the SIS data. We made spectra from a circular region with a radius of 4' near the center of each SIS chip in the mapping observations of the Galactic Center region. We then fitted each spectrum in the 4.5–10 keV band with a continuum plus three Gaussian lines fixing the center energies to be 6.4, 6.7 and 6.97 keV. The intensity ratio of the 6.7 keV to 6.97 keV lines was kept to be constant from place to place, because Maeda (1998) and Koyama et al. (1996) found no significant variation of the flux ratio. Figure 5 shows the 6.4 keV-line fluxes along positions, where the flux is converted to the value in a 2' radius, the same radius of the source region. From Figure 5, we can safely conclude that uncertainty of the iron line flux in 1E 1740.7–2942 due to the background fluctuation is less than 0.6×10^{-5} photon sec⁻¹ cm⁻²/(2'-circle). This value is, at most, 15% of that from 1E 1740.7–2942, hence can be ignored in the following discussion.

EDITOR: PLACE FIGURE 5 HERE.

4. Discussion

4.1. Absorption and Iron Abundance

The *ASCA* results of 1E 1740.7–2942 have been already reported by Churazov et al. (1996) and Sheth et al. (1996). Although they used essentially the same data sets, their results are not fully consistent with each other. The major difference is found in the N_{H} values.

With a single power-law fitting and absorption gas of solar abundance, Churazov et al. (1996) gave N_{H} to be 1.7×10^{23} H cm⁻² of the *ASCA* spectrum in the range of the 4–10 keV band, but found 1×10^{23} H cm⁻² when the full energy range of 0.4–10 keV was used. Sheth et al. (1996) estimated N_{H} to be 0.8×10^{23} H cm⁻² by the same model fitting but

in the 0.5–12 keV range. We found that the apparent inconsistency can be solved if iron is overabundant relative to the other elements. In fact, we have shown that the spectra of 1E 1740.7–2942 are well presented with a single-power model absorbed by the gas column of $1 \times 10^{23} \text{ H cm}^{-2}$, in which iron abundance is 2 solar.

Murakami et al. (1998) analyzed the reflected X-ray by the giant molecular cloud Sgr B2, which is located in nearly the same (angular) distance but in the opposite direction from the Galactic Center, and found that iron is overabundant relative to the other elements. On the other hand, Sellgren, Carr, & Balachandran (1997) and Ramirez et al. (1998), with the infrared observations of the atmosphere on the giant stars near the Galactic Center, estimated that the iron abundance relative to hydrogen is consistent with the solar value. Thus further deep observations of K-edge absorption feature of X-ray sources near the Galactic Center are required.

Sakano et al. (1999) analyzed many X-ray sources located near the Galactic Center region, and found that the N_{H} values can be well described by a simple function of the galactic latitude (Figure 2 in Sakano et al. (1999)). From their results, we estimate that the interstellar absorption to the 1E 1740.7–2942 direction is $(1\text{--}2) \times 10^{23} \text{ H cm}^{-2}$, in agreement with the best-fit N_{H} of the 1E 1740.7–2942 spectrum. No change of N_{H} during the *ASCA* long term observations implies that the absorption region should have a size larger than a few light-yrs, excluding a possibility of an accretion disk or stellar corona. Thus 1E 1740.7–2942 is very likely to be located near at the Galactic Center.

The radio observations of the large molecular cloud toward 1E 1740.7–2942, on the other hand, gave the total hydrogen column density to be $N_{\text{H}} \sim 6 \times 10^{23} \text{ H cm}^{-2}$ (Bally & Leventhal 1991; Vilhu et al. 1996). One may argue, however, that the conversion factor from the CO line intensity to the hydrogen column density may have large uncertainty. Oka et al. (1998), for example, pointed out that the usual conversion factor is not appropriate for the clouds in the Galactic Center region, and that the derived mass in the ordinary manner should be reduced by several factors. Taking this possible uncertainty into account, we still suspect that the molecular cloud is located behind 1E 1740.7–2942.

4.2. 6.4-keV iron line

We found no significant line emission from a neutral iron (6.4 keV-line). The upper-limits of the equivalent width are estimated to be a few ten eV, depending on the observation period and detector. The most stringent limit is found to be 15 eV in the combined (GIS and SIS) analysis of AO-2. These results of small equivalent width further confirm the result by Churazov et al. (1996) with larger data sets.

The equivalent width $< 15 \text{ eV}$ implies that the mean iron column density around 1E 1740.7–2942 is less than $N_{\text{Fe}} < 5 \times 10^{17} \text{ Fe cm}^{-2}$ (Inoue 1985; Awaki 1991). This value

is smaller than 1/10 of the total column density estimated from the 7.1 keV edge depth. Hence 1E 1740.7–2942 cannot be in a local dense cloud as suggested by Bally & Leventhal (1991) and Mirabel et al. (1991).

Bally & Leventhal (1991) estimated the required local density of the interstellar matter around 1E 1740.7–2942 for the observed luminosity of 1E 1740.7–2942 when it is powered directly by the interstellar matter in the case of Bondi-Hoyle accretion (Bondi & Hoyle 1944). The calculated luminosity is,

$$L = 2.3 \times 10^{36} \eta \left[\frac{M}{M_{\odot}} \right]^2 \left[\frac{v}{10 \text{ km s}^{-1}} \right]^{-3} \left[\frac{n_{\text{H}}}{10^4 \text{ cm}^{-3}} \right] \text{ (erg s}^{-1}\text{)}, \quad (1)$$

where η is the fraction of the released energy with emission from the rest mass energy, M is the mass of the central compact object, v is the relative velocity of the compact object against the cloud, and n_{H} is the hydrogen density of the cloud. The highest luminosity of 1E 1740.7–2942 in the *ASCA* observations is estimated to be 3×10^{36} erg s $^{-1}$, from the X-ray flux of 2×10^{-10} erg cm $^{-2}$ s $^{-1}$ in the 2–10 keV band and the source distance of 8.5 kpc. Since the spectrum is extracted within 2'-radius (5 pc-radius), the observed upper-limit of the iron equivalent width is converted to the local density of

$$n_{\text{H}} = 7 \times 10^2 (Z_{\text{Fe}})^{-1} \text{ (H cm}^{-3}\text{)}, \quad (2)$$

where Z_{Fe} is iron abundance relative to solar.

Then, assuming $\eta = 0.1$, we can set possible ranges of M and v for the Bondi-Hoyle accretion scenario as is given in Figure 6 with solid lines, while the dashed line shows the most probable case of $Z_{\text{Fe}} = 2$ in equation (2). Thus we find that the velocity of 1E 1740.7–2942 must be less than 10 km s $^{-1}$ even in the case of the large mass of $20M_{\odot}$ under the Bondi-Hoyle accretion scenario.

The velocity of black holes would be larger than that of normal stars due to additional kick velocity by supernova explosions. Since no data of the velocity dispersion of black holes are found, the best alternative way to estimate the velocity of 1E 1740.7–2942 is to use the velocity dispersion of neutron stars, which are also produced by supernova explosions. Thus we refer the velocity dispersion of the radio pulsars (neutron stars) (Lorimer, Bailes, & Harrison 1997; Hansen & Phinney 1997) and find that the velocity of 1E 1740.7–2942 would be larger than 10 km s $^{-1}$ with more than 99% probability. We therefore conclude that the Bondi-Hoyle scenario that 1E 1740.7–2942 is powered directly from a molecular cloud is unlikely.

EDITOR: PLACE FIGURE 6 HERE.

4.3. Long term variability

Pavlinsky et al. (1994) reported the long term variability of 1E 1740.7–2942 measured with ART-P on board *Granat*. According to their results, 1E 1740.7–2942 was usually in a medium or high state since 1990 with occasional exceptions of low state. Since the spectral shape during the *ASCA* observations showed no significant change except for the variability of the total flux, we safely assume that the spectra in the *Granat* observations has the same photon index ($\Gamma \sim 1.2$) as those of the *ASCA* spectra. Then we found that the *ASCA* fluxes of $(1\text{--}2) \times 10^{-10}$ erg cm $^{-2}$ s $^{-1}$ in the 2–10 keV band corresponds to $(2.5\text{--}5) \times 10^{-10}$ erg cm $^{-2}$ s $^{-1}$ in the 8–20 keV band, the middle to high-state fluxes of *Granat*. The *ASCA* flux is also in agreement with the BATSE light curve for the same period (Zhang et al. 1997). The similarity between the *ASCA* and BASTE light curves is another indication of the spectral invariance over larger energy range.

5. Summary

Using all the *ASCA* data of 1E 1740.7–2942, available at the time of this writing, we conclude as follows:

1. We found that 1E 1740.7–2942 was in the middle to high flux state, showing long term variation of the factor of two in a span of 3.5 years, while the photon index and column density have been nearly constant.
2. The wide band spectrum in the 1–10 keV band is well fitted with an absorbed power-law, where the iron abundance is twice as the others in a unit of solar value. The power-law slope is particularly flat with $\Gamma = 0.9\text{--}1.3$, which implies that 1E 1740.7–2942 was in the hard state. The large hydrogen column density of $N_{\text{H}} \sim 1 \times 10^{23}$ H cm $^{-2}$ supports the location of 1E 1740.7–2942 to be near the Galactic Center.
3. From the iron-edge structure we estimated the iron column density to be $N_{\text{Fe}} \sim 1 \times 10^{19}$ Fe cm $^{-2}$.
4. The iron equivalent width has been very small with the upper-limit of 15 eV. This indicates that the iron column near around 1E 1740.7–2942 is less than $N_{\text{Fe}} < 5 \times 10^{17}$ Fe cm $^{-2}$.
5. Our results favor the geometry that 1E 1740.7–2942 is not in the radio molecular cloud. The cloud would be, by chance, in the line of sight to, or possibly behind 1E 1740.7–2942. This indicates that the X-ray emission does not originate by the direct accretion from the molecular cloud. 1E 1740.7–2942 is probably a normal black hole binary.

The authors express their thanks to all of the members of the *ASCA* team whose efforts made these observations and data analysis possible. We are grateful to Dr. S. Yamauchi, Prof. Ph. Durouchoux, and, particularly, an anonymous referee for their valuable comments and suggestions. M. S. thanks to Drs. H. Sogawa, M. Ozaki, Y. Fujita and H. Matsumoto for discussion. M. S. and Y. M. acknowledge the supports from the Japan Society for the Promotion of Science for Young Scientists.

REFERENCES

Anders, E., & Grevesse, N. 1989, *Geochimica et Cosmochimica Acta*, 53, 197

Awaki, H. 1991, Ph.D. thesis, Nagoya University

Bally, J., & Leventhal, M. 1991, *Nature*, 353, 234

Bałucińska-Church, M., & McCammon, D. 1992, *ApJ*, 400, 699

Bazzano, A., La Padula, C., Ubertini, P., & Sood, R. K. 1992, *ApJ*, 385, L17

Bondi, J., & Hoyle, F. 1944, *MNRAS*, 104, 21

Bouchet, L., et al. 1991, *ApJ*, 383, L45

Burke, B. E., Mountain, R. W., Harrison, D. C., Bautz, M. W., Doty, J. P., Ricker, G. R., & Daniels, P. J. 1991, *IEEE Trans. ED-38*, 1069

Burke, B. E., Mountain, R. W., Daniels, P. J., & Dolat, V. S. 1994, *IEEE Trans. Nuc. Sci.*, 41, 375

Cheng, L. X., Leventhal, M., Smith, D. M., Gehrels, N., Tueller, J., & Fishman, G. 1998, *ApJ*, 503, 809

Churazov, E., et al. 1993a, *A&AS*, 97, 173

Churazov, E., et al. 1993b, *ApJ*, 407, 752

Churazov, E., Gilfanov, M., & Sunyaev, R. 1996, *ApJ*, 464, L71

Cook, W. R., Grunsfeld, J. M., Heindl, W. A., Palmer, D. M., Prince, T. A., Schindler, S. M., & Stone, E. C. 1991, *ApJ*, 372, L75

Cordier, B., et al. 1993a, *A&A*, 275, L1

Cordier, B., et al. 1993b, *A&A*, 272, 277

Djorgovski, S., Thompson, D., Mazzarella, J., Klemola, A., Neugebauer, G., Matthews, K., & Armus, L. 1992, *IAU Circ.* No. 5596

Fender, R. P., Burnell, S. J. B., & Waltman, E. B. 1997, *Vistas in Astronomy*, 41, 3

Goldwurm, A., et al. 1994, *Nature*, 371, 589

Hansen, B. M. S., & Phinney, E. S. 1997, *MNRAS*, 291, 569

Harris, M. J., Share, G. H., & Leising, M. D. 1994a, *ApJ*, 420, 649

Harris, M. J., Share, G. H., & Leising, M. D. 1994b, *ApJ*, 433, 87

Heindl, W. A., Prince, T. A., & Grunsfeld, J. M. 1994, *ApJ*, 430, 829

Hertz, P., & Grindlay, J. E. 1984, *ApJ*, 278, 137

Inoue, H. 1985, *Space Science Reviews*, 40, 317

Jung, G. V., et al. 1995, *A&A*, 295, L23

Kawai, N., Fenimore, E. E., Middleditch, J., Cruddace, R. G., Fritz, G. G., Snyder, W. A., & Ulmer, M. P. 1988, *ApJ*, 330, 130

Koyama, K., Maeda, Y., Sonobe, T., Takeshima, T., Tanaka, Y., & Yamauchi, S. 1996, *PASJ*, 48, 249

Kuznetsov, S., et al. 1997, *MNRAS*, 292, 651

Lorimer, D. R., Bailes, M., & Harrison, P. A. 1997, *MNRAS*, 289, 592

Maeda, Y. 1998, Ph. D. thesis, Kyoto University

Makishima, K., et al. 1996, *PASJ*, 48, 171

Malet, I., et al. 1995, *ApJ*, 444, 222

Mereghetti, S., Caraveo, P., Bignami, G. F., & Belloni, T. 1992, *A&A*, 259, 205

Mirabel, I. F., Paul, J., Cordier, B., Morris, M., & Wink, J. 1991, *A&A*, 251, L43

Mirabel, I. F., Rodríguez, L. F., Cordier, B., Paul, J., & Lebrun, F. 1992, *Nature*, 358, 215

Mirabel, I. F., Rodríguez, L. F., Cordier, B., Paul, J., & Lebrun, F. 1993, *A&AS*, 97, 193

Murakami, H., Koyama, K., Sakano, M., Tsujimoto, M., & Maeda, Y. 1998, in preparation

Ohashi, T., et al. 1996, *PASJ*, 48, 157

Oka, T., Hasegawa, T., Hayashi, M., Handa, T., & Sakamoto, S. 1998, *ApJ*, 493, 730

van Paradijs, J. 1998, Neutron Stars and Black Holes in X-Ray Binaries, in “The Many Faces of Neutron Stars”, eds. R. Buccieri, J. van Paradijs, & M. A. Alpar (London: Kluwer Academic Publishers), in press

Paciesas, W. S., Harmon, B. A., Pendleton, G. N., Finger, M. H., Fishman, G. J., Meegan, C. A., Rubin, B. C., & Wilson, R. B. 1993, *A&AS*, 97, 253

Pavlinsky, M. N., Grebenev, S. A., & Sunyaev, R. A. 1994, *ApJ*, 425, 110

Prince, T., Skinner, G., Kulkarni, S. R., Matthews, K., & Neugebauer, G. 1991, IAU Circ. No. 5252

Ramirez, S. V., Sellgren, K., Carr, J. S., Balachandran, S. C., Blum, R. D., & Terndrup, D. 1998, in proc of “The Central Parsecs — Galactic Center Workshop ’98”, in press

Sakano, M., Koyama, K., Nishiuchi, M., Yokogawa, J., & Maeda, Y. 1999, Advances in Space Research, in press

Sellgren, K., Carr, J. S., & Balachandran, S. C. 1997, IAU Symp. 184, The Central regions of the Galaxy and Galaxies, ed. Y. Sofue (London: Kluwer Academic Publishers), 21

Serlemitsos, P. J., et al. 1995, PASJ, 47, 105

Sheth, S., Liang, E., Luo, C., & Murakami, T. 1996, ApJ, 468, 755

Skinner, G. K., Willmore, A. P., Eyles, C. J., Bertram, D., & Church, M. J. 1987, Nature, 330, 544

Skinner, G. K., et al. 1991, A&A, 252, 172

Smith, D. M., Leventhal, M., Cavallo, R., Gehrels, N., Tueller, J., & Fishman, G. 1996, ApJ, 458, 576

Smith, D. M., Heindl, W. A., Swank, J., Leventhal, M., Mirabel, I. F., & Rodríguez, L. F. 1997, ApJ, 489, L51

Sunyaev, R., et al. 1991, ApJ, 383, L49

Tanaka, Y., Inoue, H., & Holt, S. S. 1994, PASJ, 46, L37

Tanaka, Y., & Lewin, W. H. G. 1995, in X-ray Binaries, eds. W. H. G. Lewin, J. van Paradijs, & E. P. J. van den Heuvel (New York: Cambridge University Press), 126

Vilhu, O., Hannikainen, D., Muhli, P., Huovelin, J., Poutanen, J., Durouchoux, Ph., & Wallyn, P. 1996, in proc of 2nd INTEGRAL workshop “The Transparent Universe”

Yamashita, A., et al. 1997, IEEE Trans. Nucl. Sci., 44, 847

Yokogawa, J., Sakano, M., Koyama, K., & Yamauchi, S. 1998, Advances in Space Research, submitted

Zhang, S. N., Harmon, B. A., & Liang, E. P. 1997, in proc of the Fourth Compton Symposium, eds. Dermer, C. D., Strickman, M. S., & Kurfess, J. D. (The American Institute of Physics), 410, 873

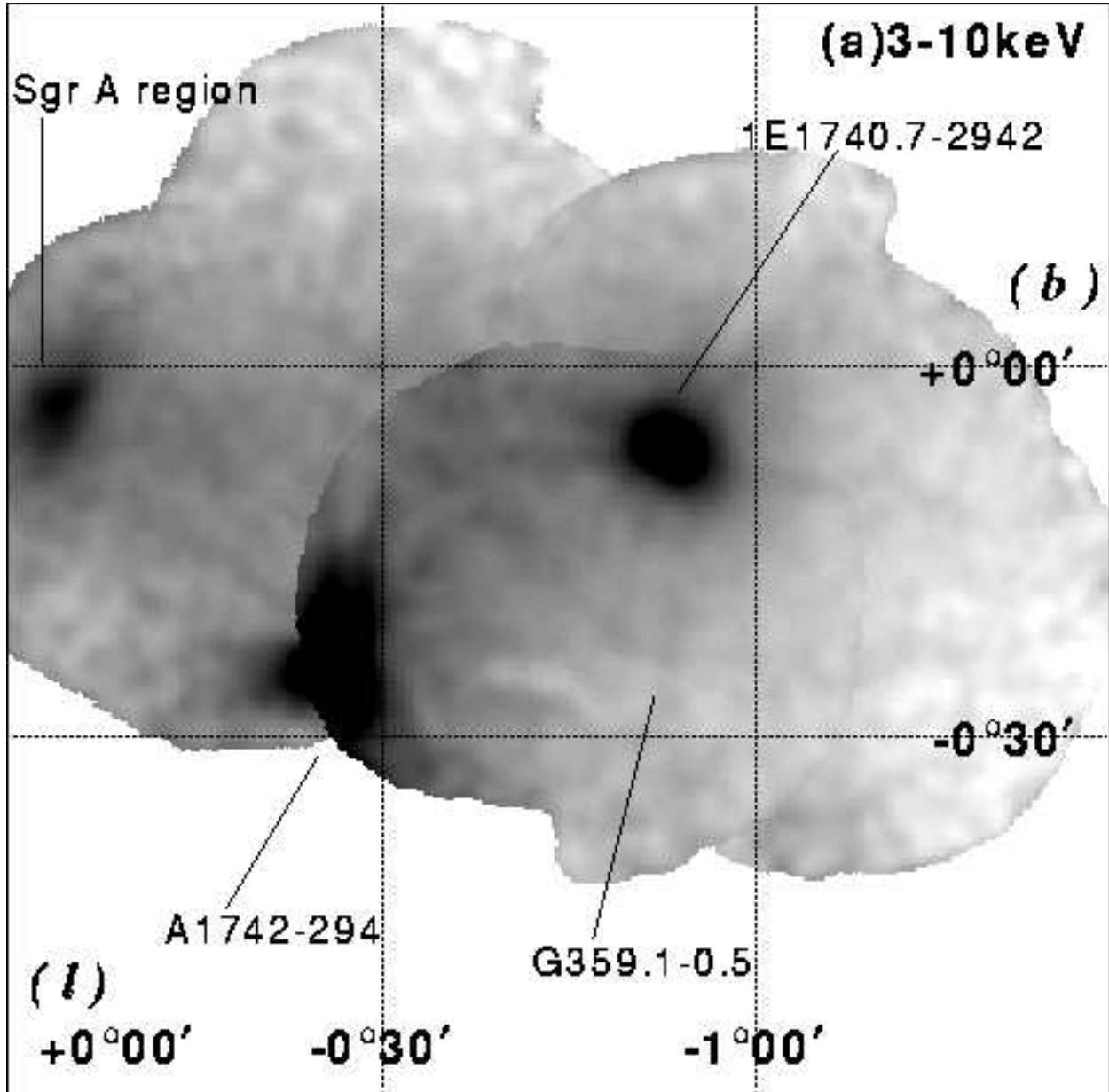


Fig. 1.— The GIS mosaic images near 1E 1740.7–2942; (a) in the 3–10 keV band, (b) in the 0.7–1.5 keV band. The images are taken with multiple pointings of *ASCA* in 1993–1997. The data of GIS2 and GIS3 are summed, smoothed with a Gaussian filter of $\sigma = 3$ pixels (~ 0.75 arcmin), and corrected for exposure, vignetting and the detection efficiency with GIS grid, after non X-ray background is subtracted. The dotted grids are the galactic coordinate ($l_{\text{II}}, b_{\text{II}}$). Color levels are logarithmically spaced. The stray lights by some bright sources, which are variable from epoch to epoch, make images complicated, for example, they make images discontinuous on the edges of the fields of views. A faint soft source, AX J1744.3–2940, at $(17^{\text{h}}44^{\text{m}}18^{\text{s}}, -29^{\circ}40.1')$ in J2000 coordinate is found. The positions of Sgr A region and SNR G359.1–0.5 (Yokogawa et al. 1998) are also indicated.

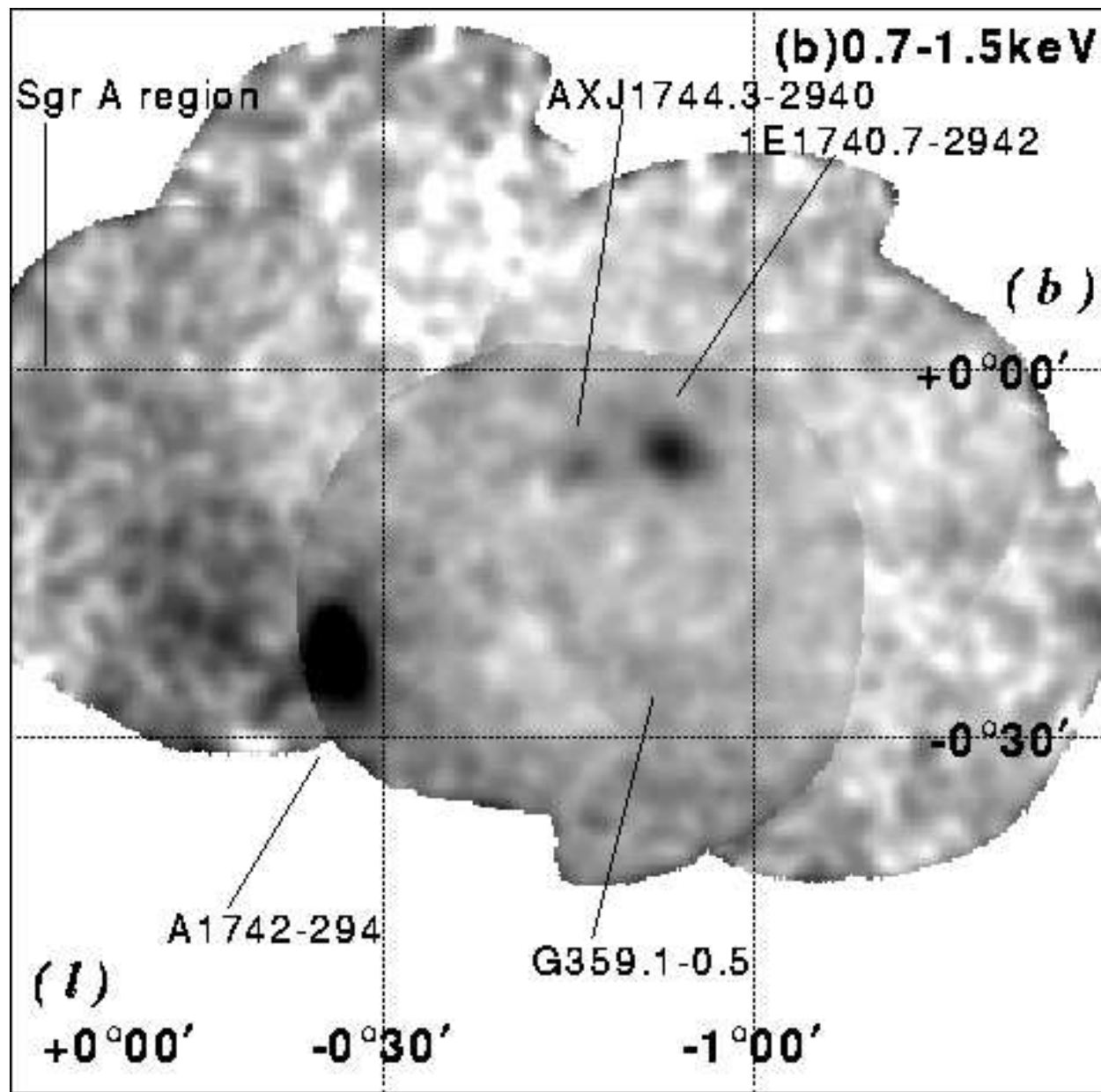


Fig. 1.— (b)

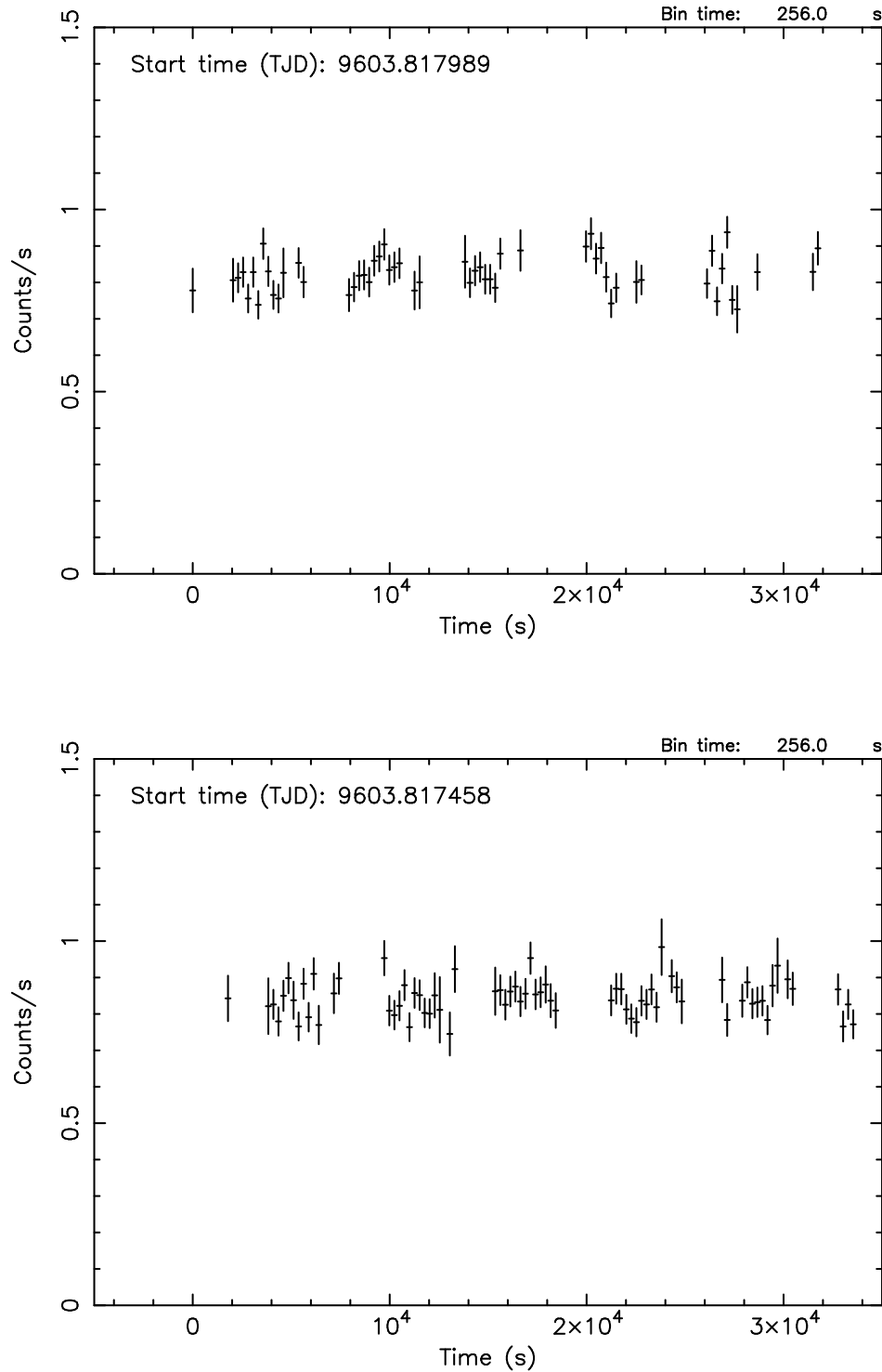


Fig. 2.— The 2–10 keV light curves with 256 second bin for the AO-2 1st observation: (left) GIS 2+3 data and (right) SIS 0+1.

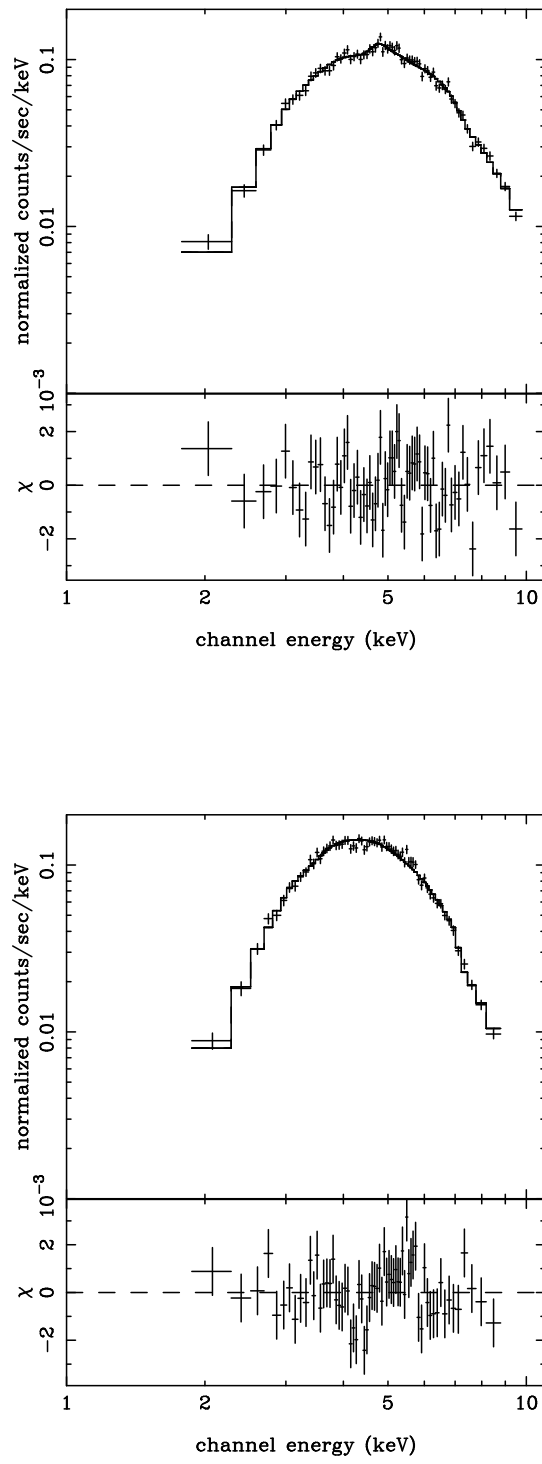


Fig. 3.— The spectra of AO-2 with the best-fit model (solid lines): (left) GIS 2+3 and (right) SIS 0+1.

Long term variability of 1E 1740.7–2942

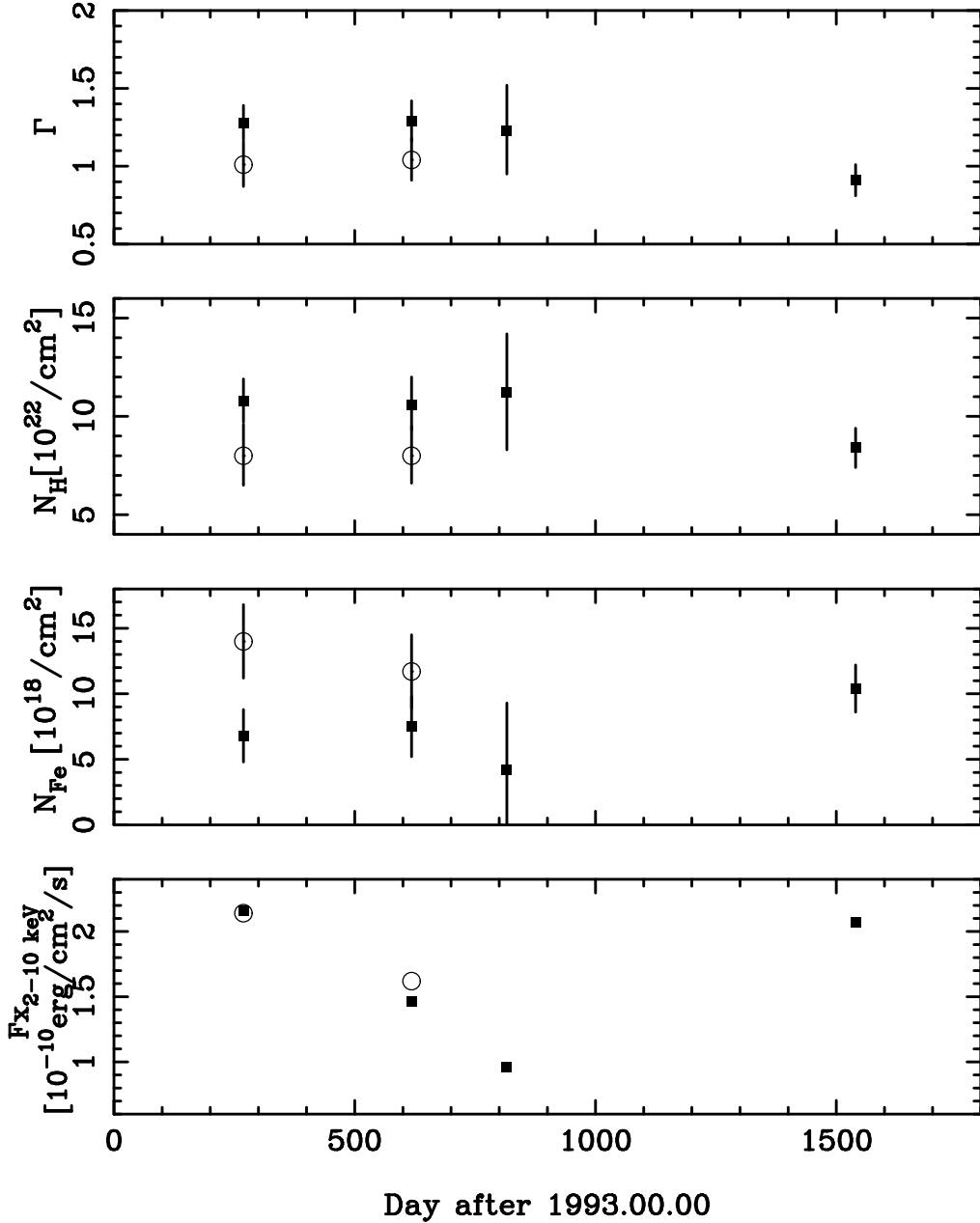


Fig. 4.— Long term variability of a power-law photon index Γ , hydrogen column density N_H in unit of $10^{22} \text{ H cm}^{-2}$, iron column density N_{Fe} in unit of $10^{18} \text{ Fe cm}^{-2}$ and the X-ray flux in the 2–10 keV band F_X in unit of $10^{-10} \text{ erg cm}^{-2} \text{ s}^{-1}$. Close boxes and open circles represent the data taken in GIS and SIS, respectively.

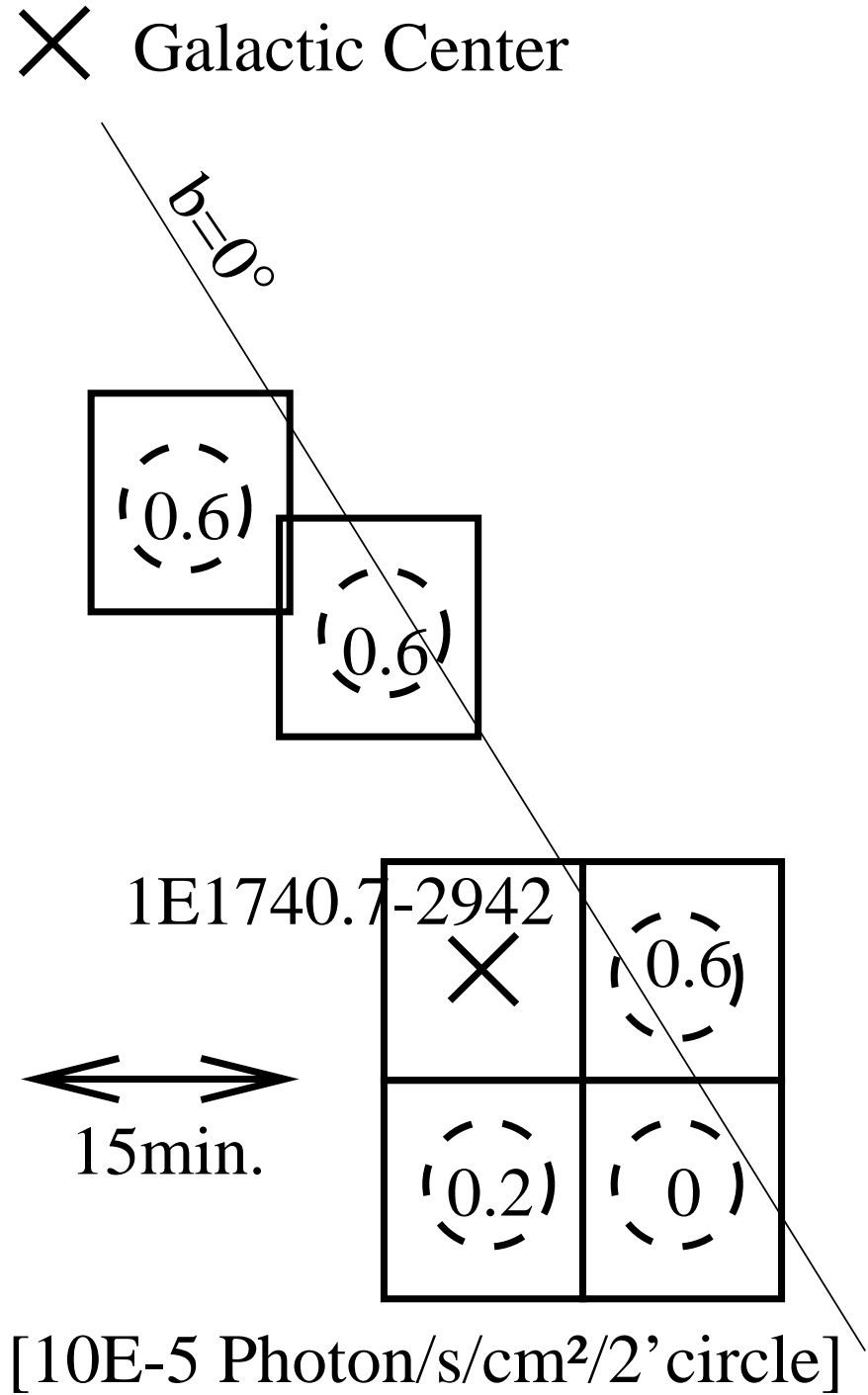


Fig. 5.— Iron line distribution in the Galactic Center region near 1E 1740.7–2942 estimated by a spectral analysis in a 4' radius circle of each SIS chip for the data taken in 1993 (see Table 1). The best-fit flux of the neutral iron 6.4 keV line is normalized to the value in a 2' radius region with an assumption of the uniform distribution of diffuse 6.4 keV line in the circle. These are given in the circles on the figure with the unit of 10^{-5} photon s^{-1} cm^{-2} /(2' radius circle).

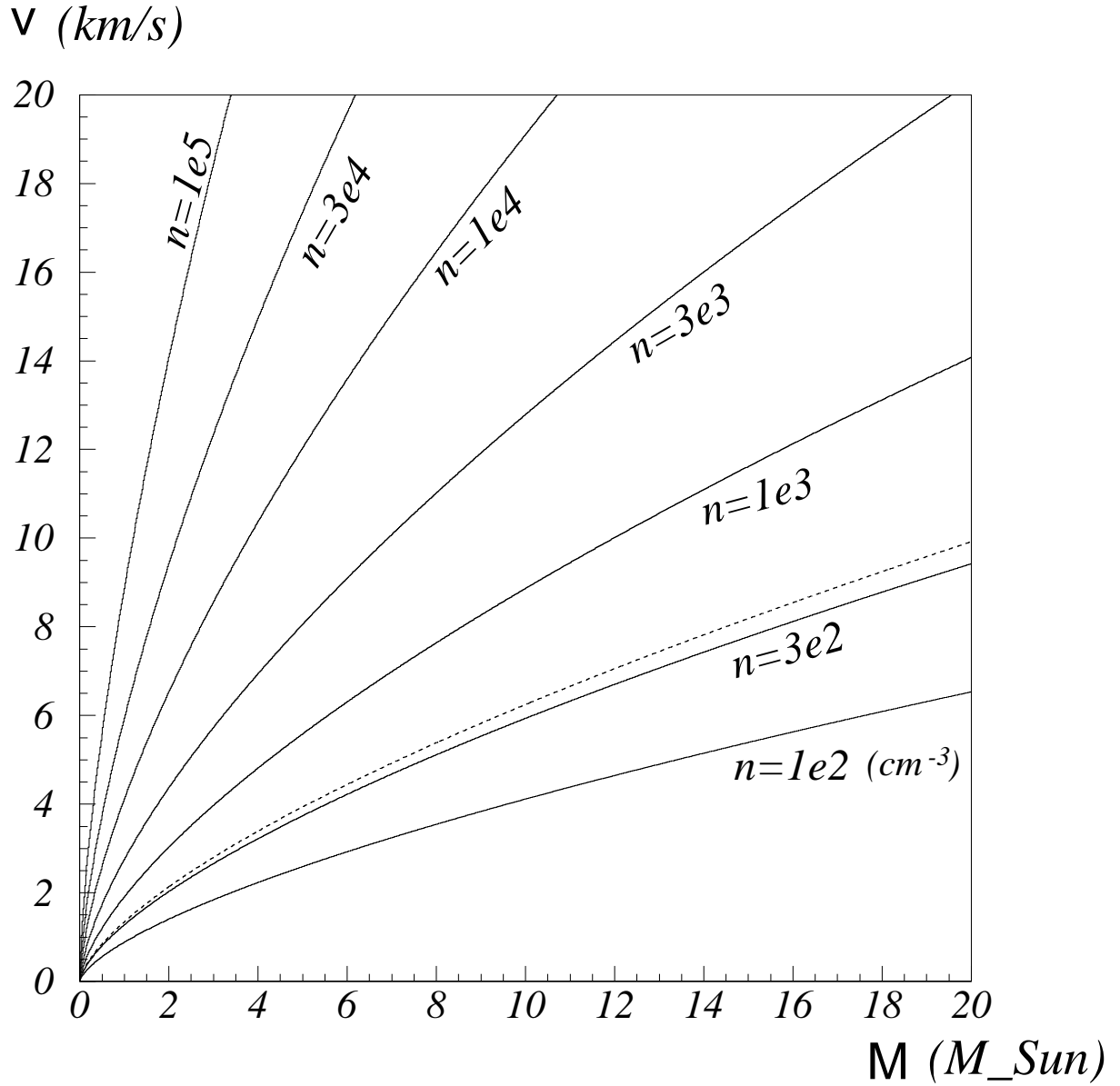


Fig. 6.— The relation between the mass (M) and the velocity (v) of the central source for certain cloud density (n) to explain the observed luminosity of 1E 1740.7–2942 in the Bondi-Hoyle scenario (solid lines). The dashed line shows the case of the estimated upper limit of the density (eq. [2] with $Z_{\text{Fe}} = 2$).

Table 1: Observational log.

| Phase | Date ^a | R.A. ^b | DEC. ^b | Bit-Rate | Data Mode | | Exposure ^c | |
|-------------------|-------------------|---|-------------------|----------|-----------|-------------|-----------------------|-----|
| | | | | | GIS | SIS | GIS | SIS |
| PV | 1993/09/26 | $17^{\text{h}}43^{\text{m}}30^{\text{s}}$ | $-29^{\circ}50'$ | High | PH | 4CCD Faint | 24 | 24 |
| | | | | Medium | PH | 1CCD Bright | 10 | 12 |
| PV ^d | 1993/10/03 | $17^{\text{h}}45^{\text{m}}30^{\text{s}}$ | $-29^{\circ}14'$ | High | PH | 4CCD Faint | 8 | 6 |
| | | | | Medium | PH | 4CCD Bright | 15 | 14 |
| PV ^d | 1993/10/04 | $17^{\text{h}}44^{\text{m}}00^{\text{s}}$ | $-29^{\circ}20'$ | High | PH | 4CCD Faint | 18 | 12 |
| | | | | Medium | PH | 4CCD Bright | 3 | 3 |
| AO-2 | 1994/09/08 | $17^{\text{h}}43^{\text{m}}30^{\text{s}}$ | $-29^{\circ}50'$ | High | PH | 2CCD Faint | 12 | 12 |
| | | | | Medium | PH | 1CCD Faint | 5 | 5 |
| AO-2 | 1994/09/12 | $17^{\text{h}}43^{\text{m}}30^{\text{s}}$ | $-29^{\circ}50'$ | High | PH | 2CCD Faint | 9 | 9 |
| | | | | Medium | PH | 1CCD Faint | 4 | 4 |
| AO-3 ^e | 1995/03/27 | $17^{\text{h}}44^{\text{m}}10^{\text{s}}$ | $-30^{\circ}03'$ | High | PH | — | 24 | — |
| | | | | Medium | PH | — | 16 | — |
| AO-5 ^e | 1997/03/21 | $17^{\text{h}}44^{\text{m}}59^{\text{s}}$ | $-29^{\circ}46'$ | High | PH | — | 37 | — |
| | | | | Medium | PH | — | 49 | — |

^ayear/month/day, in Universal Time.

^bCoordinate of detector center (J2000).

^cunit of kilo-second.

^dThese pointings do not include 1E 1740.7–2942 in their fields of view. They are used for background estimation in Sec. 3.3.

^e1E 1740.7–2942 is out of the SIS fields of view.

Table 2: Best-fit parameters in the fitting with a power-law function

| Phase | | Absorbed Power-law Model | | | | $\chi^2/\text{d.o.f.}$ | F_X^e | 6.4 keV-line Inclusive | |
|-------|---------|--------------------------|---------------------|----------------------|---------------------|------------------------|---------|------------------------|------------------------|
| | | Γ^a | $I_{1\text{keV}}^b$ | N_H^c | N_{Fe}^d | | | $L_{6.4\text{keV}}^f$ | $EW_{6.4\text{keV}}^g$ |
| PV | GIS | 1.28 ± 0.11 | $4.8_{-0.9}^{+1.1}$ | 10.8 ± 1.1 | 6.7 ± 2.0 | 89.2/69 | 2.16 | 6 ± 8 | 17 ± 22 |
| | SIS | $1.01_{-0.14}^{+0.15}$ | $3.0_{-0.7}^{+1.0}$ | $8.0_{-1.5}^{+1.6}$ | 14.0 ± 2.8 | 136.4/115 | 2.14 | 5 ± 7 | 13 ± 18 |
| | GIS+SIS | 1.18 ± 0.09 | $4.0_{-0.6}^{+0.7}$ | 9.8 ± 0.9 | 9.3 ± 1.6 | 256.0/188 | 2.15 | 5 ± 5 | 13 ± 14 |
| AO-2 | GIS | 1.29 ± 0.13 | $3.3_{-0.7}^{+1.0}$ | $10.6_{-1.3}^{+1.4}$ | 7.5 ± 2.3 | 73.4/63 | 1.46 | < 6.3 | < 25 |
| | SIS | $1.04_{-0.13}^{+0.14}$ | $2.3_{-0.5}^{+0.7}$ | $8.0_{-1.4}^{+1.5}$ | 11.7 ± 2.8 | 75.4/63 | 1.62 | < 4.8 | < 17 |
| | GIS+SIS | 1.24 ± 0.09 | $3.2_{-0.5}^{+0.6}$ | 9.8 ± 1.0 | $9.1_{-1.7}^{+1.8}$ | 238.9/130 | 1.51 | < 4.3 | < 15 |
| AO-3 | GIS | $1.23_{-0.28}^{+0.29}$ | $2.0_{-0.8}^{+1.4}$ | $11.2_{-2.9}^{+3.0}$ | 4 ± 5 | 46.6/44 | 0.96 | < 9 | < 56 |
| AO-5 | GIS | 0.91 ± 0.10 | $2.3_{-0.4}^{+0.5}$ | 8.4 ± 1.0 | 10.4 ± 1.8 | 131.6/89 | 2.07 | 0.7 ± 7 | 2 ± 20 |

^aPhoton index.

^bIntensity of continuum at 1keV [10^{-2} photon $\text{keV}^{-1} \text{ cm}^{-2} \text{ s}^{-1}$] (absorption corrected).

^cHydrogen column density [$10^{22} \text{ H cm}^{-2}$].

^dIron column density [$10^{18} \text{ Fe cm}^{-2}$].

^eObserved flux with 2–10 keV [$10^{-10} \text{ erg cm}^{-2} \text{ s}^{-1}$].

^fLuminosity of 6.4keV-line [$10^{-5} \text{ Photon cm}^{-2} \text{ s}^{-1}$] (absorption corrected).

^gEquivalent width of 6.4 keV-line [eV].